Structural Engineering and Mechanics, Vol. 32, No. 2 (2009) 283-300
DOI: http://dx.doi.org/10.12989/sem.2009.32.2.283

Validation study on numerical simulation of RC response to close-in blast with a fully coupled model

Shunfeng Gong†

Institute of Structural Engineering, College of Civil Engineering and Architectural, Zhejiang Univ., 310058, P.R. China

Yong Lu‡ and Zhenguo Tu‡†

Institute for Infrastructure and Environment, School of Engineering, University of Edinburgh, Edinburgh EH9 3JL, UK

Weiliang Jin‡‡

Institute of Structural Engineering, College of Civil Engineering and Architectural, Zhejiang Univ., 310058, P.R. China

(Received November 25, 2008, Accepted March 19, 2009)

Abstract. The characteristic response of a structure to blast load may be divided into two distinctive phases, namely the direct blast response during which the shock wave effect and localized damage take place, and the post-blast phase whereby progressive collapse may occur. A reliable post-blast analysis depends on a sound understanding of the direct blast effect. Because of the complex loading environment and the stress wave effects, the analysis on the direct effect often necessitates a high fidelity numerical model with coupled fluid (air) and solid subdomains. In such a modelling framework, an appropriate representation of the blast load and the high nonlinearity of the material response is a key to a reliable outcome. This paper presents a series of calibration study on these two important modelling considerations in a coupled Eulerian-Lagrangian framework using a hydrocode. The calibration of the simulated blast load is carried out for both free air and internal explosions. The simulation of the extreme dynamic response of concrete components is achieved using an advanced concrete damage model in conjunction with an element erosion scheme. Validation simulations are conducted for two representative scenarios; one involves a concrete slab under internal blast, and the other with a RC column under air blast, with a particular focus on the simulation sensitivity to the mesh size and the erosion criterion.

Keywords: blast load; concrete component; numerical simulation; Eulerian solver; Lagrangian solver; hydrocode; mesh sensitivity.

† Associated Professor, E-mail: sfgong@zjuem.zju.edu.cn
‡ Professor, Corresponding author, E-mail: yong.lu@ed.ac.uk
‡† Ph.D., E-mail: zgtucareer@yahoo.com
‡‡ Professor, E-mail: jinwl@zju.edu.cn

1. Introduction

Analysis of structures against explosive loading has been a subject of extensive study in recent years due to concerns over infrastructure securities as well as advancing the technology in modern protective designs. Apart from simplified analytical approaches, such as those based on advanced single-degree-of-freedom (SDOF) systems and beam-column approximations (e.g., Krauthammer *et al.* 2003, Gong and Lu 2007), there is a trend of increasing use of advanced numerical models to perform high fidelity simulations to obtain more realistic and detailed response predictions, especially for the direct blast effects (e.g., Gebbeken and Ruppert 1999, Xu and Lu 2006, Leppanen 2006, Rabczuk and Eibl 2006).

Despite the availability of a range of numerical modelling options, to conduct a sound numerical simulation of concrete structures under explosive loading is not a straightforward task due to a number of complex phenomena involved. Among other considerations, a reliable simulation must ensure accurate reproduction of the explosive loading, adequate transfer of the blast load onto the structure, and a sound description of the material response which often involves severe deformations. These requirements are particularly important for the simulation of close-in explosions, as in such cases both the loading environment and the structural response would exhibit drastic spatial and time variations, and hence the response could be highly sensitive to the accuracy in the modelling of the load and the material behaviour.

In a close-in explosion situation, the presence of a solid object can significantly affect the propagation of the air blast. Therefore, it would be very difficult to define accurately the blast load on the solid structure using an empirical method. To resolve this problem would generally require a full coupled computational model, in which both the charge detonation in air and the response of the solid structure are explicitly modelled while an appropriate coupling algorithm is applied between the air (fluid) and the solid structure. The present study mainly concerns such a fully coupled modelling scheme, with a particular focus on the simulation of concrete structures using a general purpose hydrocode (LS-DYNA 2003).

On the blast load simulation, previous experiences have shown that in the close-in range the simulation of the blast load from explosive charge detonation can be quite sensitive to the configuration of the numerical model and the mesh size, as well as the interface setting between the air blast and the solid structure. To examine these modelling factors, a series of blast load simulations have been carried out, and a summary of the simulation and the outcome is given in the first part of this paper. Different mesh sizes are explored and the trend of convergence of the blast parameters is scrutinized. The simulation results in the free air are benchmarked against the empirical data available in TM5-1300 (1990).

On the modelling of concrete material under high rate loading, a number of studies have been conducted in the past in attempt to establish a rational theory on the damage and fragmentation mechanisms of brittle materials subjected to high rate loading (e.g., Hommert *et al.* 1987, Brinkman 1987). Continuous improvement is being achieved in the material constitutive models for high dynamic loads (Holmquist 1993, Malvar *et al.* 1997, Gebbeken and Ruppert 2000, Gatuingt and Pijaudier-Cabot 2002). It is also recognized that even with a robust material model, a proper choice of the model parameter values can play a significant role in determining the actual performance of the model (Lu and Tu 2009). In the present study, the concrete damage model proposed by Malvar *et al.* (1997, 2000) is employed. To tackle the numerical problem caused by large deformations in a mesh-based FE model, an erosion technique is employed by deleting the severely distorted

elements. Such an approach is also seemingly applicable for the simulation of cracks in concrete structures. In such a scheme, the criterion for the element erosion can be a controversial subject and this paper will provide a recommendation in this regard through representative simulation studies.

2. Calibration of blast load simulation for coupled analysis using LS-DYNA

2.1 Calibration of blast load simulation in free air

Blast in free air is a basic scenario that a hydrocode-oriented numerical model should be capable of reproducing in the first place. In this study, the simulation of blast in free air, using LS-DYNA (2003), is examined first. It is worth noting that LS-DYNA adopts the Arbitrary Lagrangian-Eulerian (ALE) method for the analysis of problems involving large deformations. When modelling explosion in free air, the method calculates the pressure profile throughout the ALE mesh.

Although theoretically speaking the simulation of the explosion of a spherical charge in free air may be simplified as a one-dimensional problem, in the current calibration analysis a three-dimensional model is considered. This is to ensure that the verification results are representative of an explosion simulation in a general 3D environment. Fig. 1 shows the general numerical model mesh configuration. Because of symmetry (considering a generic cubic charge), a one-eighth symmetrical model is constructed. Appropriate boundary conditions to constrain motion normal to the symmetric planes are applied on the XY, XZ, and YZ planes, which intersect at the centre of the charge. The remaining three boundary planes are set as non-reflective boundary to simulate the actual continuity of the air medium.

In the numerical model, the detonation of the charge is modelled by the empirical Jones-Wilkins-Lee (JWL) equation of state (EOS) (Lee *et al.* 1968), while a linear polynomial equation of state is used to simulate the air. During the computation, the overpressure time histories at selected locations in the air medium are recorded. The maximum peak overpressure, duration and impulse of the airblast during the positive phase are evaluated from the overpressure time history results.

Empirical predictions are considered as benchmark for comparison with the numerical simulation results. In empirical approaches, the scaling laws are usually used to predict the properties of blast

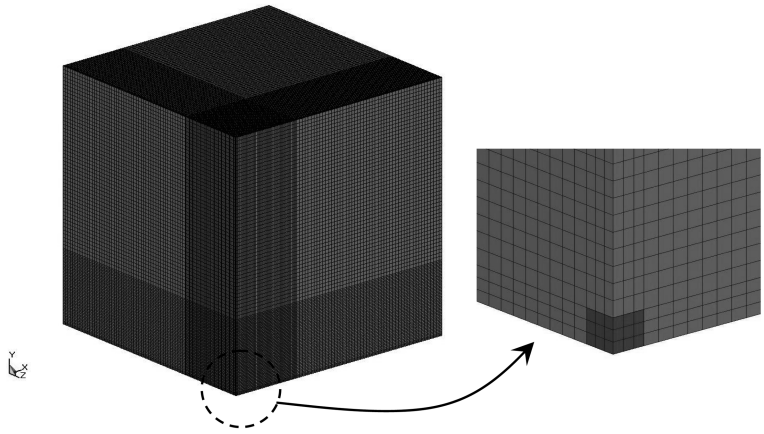

Fig. 1 Numerical model configuration for explosive detonation in free air (one-eighth symmetrical model)

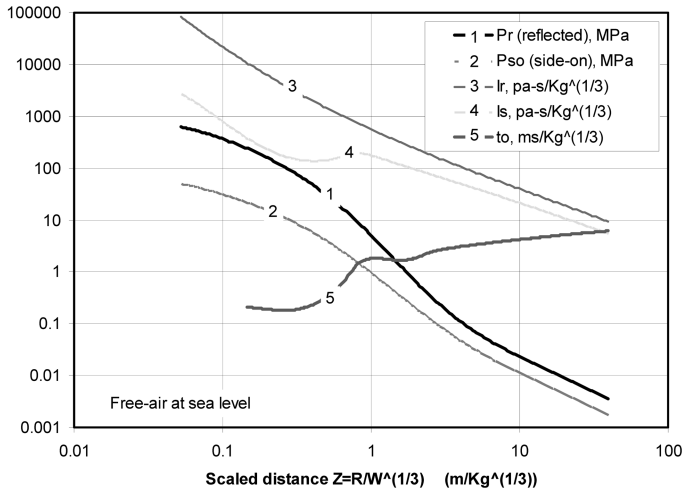

Fig. 2 Positive phase airblast parameters for a spherical TNT detonation in free air at sea level (based on TM5-1300)

waves from different charge quantities. The most common form of blast scaling is the Hopkinson-Cranz or cube-root scaling (Baker 1973), in which the scaled distance Z is introduced as $Z = R/W^{1/3}$, where R is the actual distance from the centre of the explosion to a given location (m), and W is the weight of explosive (kg). Various empirical relationships exist, for example Henrych (1979), TM5-1300 (1990). In the present calibration, the empirical data available in TM5-1300 are used for comparison with the numerical results. Fig. 2 depicts a set of empirical curves for the positive-phase free-air blast parameters based on TM5-1300.

To simplify the parametric settings, in the mesh sensitivity study a standard charge of 1 kg TNT is used, while the mesh grid size for the air is varied in a range from 0.05 m down to 0.01 m. The results, as implied by the scaling law and also confirmed by trial analyses, however, can be directly extrapolated to other charge yields if the dimensions are looked upon in scaled terms. In other words, the results from the standard 1-kg is representative of a case with a W-kg charge where the mesh grid size varies in $(0.01\sim0.05) \times W^{1/3}$ m and the blast parameters is measured at a distance of $R \times W^{1/3}$ m.

The simulated results, represented by the peak overpressure and impulse, for different mesh grid sizes are shown in Fig. 3 in comparison with the empirical predictions using TM5-1300.

As can be seen, the overpressure appears to be rather sensitive to the mesh grid size, and does not show a clear convergence trend even when the mesh grid size is being refined to a 10 mm level for the 1-kg charge scenario. On the other hand, the impulse appears to be relatively less sensitive to the mesh grid sizes in the range explored. The simulation results also indicate that both overpressure and impulse exhibit large variation with respect to the change in the mesh grid size, especially in the 0.2-0.8 m distance range. For example, at R equal to 0.5 m (or 0.5 m/kg$^{1/3}$ in scaled term), the computed impulse using 10 mm mesh is around 3 times of that using 50 mm mesh. When R is greater than 0.8 m, the difference of impulse values predicted by the model using different mesh sizes appears to be less pronounced, with a variation within about 25% from that using the 10 mm mesh size.

In general, the simulated results are observed to consistently underestimate both the peak

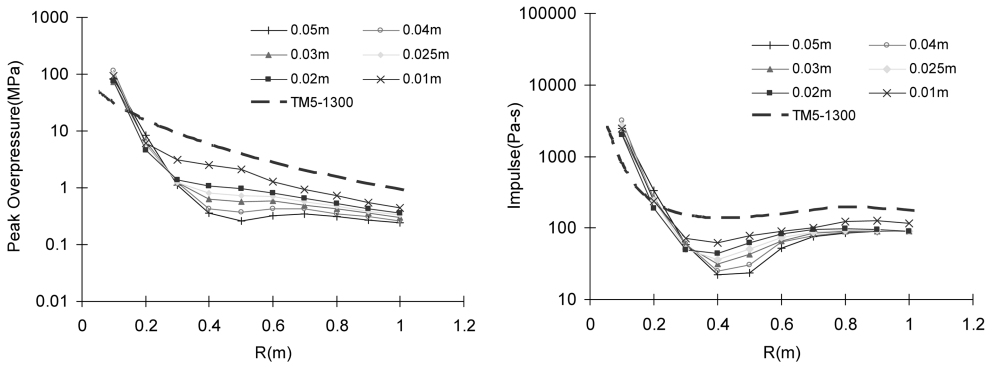

(a) Peak overpressure (b) Impulse

Fig. 3 Comparison of simulated blast load parameters using different mesh sizes with empirical data from TM5-1300

overpressure and the impulse as compared to TM5-1300, although with the refinement of the mesh the simulated results tend to improve continuously. Even with the finest mesh used, which may be regarded as reaching a limit for practical applications, the simulated results are still significantly lower than the empirical data. For example, the impulse values for the finest mesh are still only about 50% of the empirical values given by TM5-1300.

There could be other causes than the mesh size effect to the underestimation of blast load in the numerical simulation. These may include limitation of the numerical algorithms involved and approximation of air as an ideal gas, which can be particularly problematic in the vicinity of the detonation. Several options have been explored in an attempt to improve the simulation results concerning the blast load simulation within LS-DYNA, for example by modifying the EOS for the air in a certain range. The improvement was marginal. Given the fact that the simulated blast load is consistently lower, imposing an enhancement factor on the TNT explosive weight appears to be an effective alternative in lieu of a more rigorous physics-based solution. Fig. 4 shows the simulated blast load parameters considering different charge enhancement factors (1.0~3.0). For practicality, a reasonably fine mesh is used in all the simulations, and the mesh grid size is 0.02 m (or 0.02 m/kg$^{1/3}$

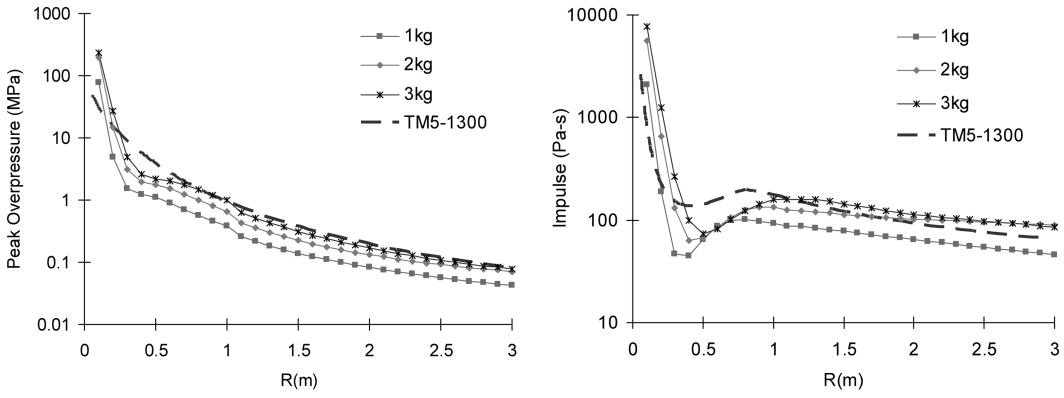

(a) Overpressure (b) Impulse

Fig. 4 Simulated peak overpressure and impulse considering a charge enhancement factor

in scaled terms) for the area within 1 m from the charge centre, and it increases to 50 mm for the remaining range.

From the results shown in Fig. 4, it may be deduced that, for a mesh gird size similar to that used in the current simulation, a charge enhancement factor of order of 2~3 may be considered as appropriate in a simulation in order to achieve a reasonably accurate reproduction of both the peak overpressure and the impulse.

2.2 A brief comparison of the free air blast simulation using AUTODYN

For the purpose of a reference comparison, the blast load generated by the detonation of high explosive charges in free air is also simulated using hydrocode AUTODYN (2001). Both an ordinary GBeta algorithm and an enhanced FCT (Flux Corrected Technique) available within AUTODYN are employed. The mesh grid size adopted is identical to that used in LS-DYNA simulations for Fig. 4. Fig. 5 shows a comparison between the simulated results using AUTODYN and the empirical counterpart from TM5-1300.

Comparing to the results obtained using LS-DYNA, the AUTODYN Euler-FCT solver appears to yield better blast load simulation both in terms of the peak overpressure and the impulse. However, certain degree of underestimation of the blast load still exists, mainly for larger scaled distance range (i.e., above 1.0 m/kg$^{1/3}$). It should also be noted that using the normal GBeta algorithm in AUTODYN the simulated air blast load exhibits a similar level of gross underestimation as with LS-DYNA.

It is therefore advisable that a blast load calibration be conducted before a comprehensive numerical study is being carried out. This would help determine the accuracy in the simulated blast load under the particular mesh and model settings, thus assisting in the interpretation of the final simulation results.

2.3 Simulation of blast load in closed space with coupled air-structure model

For internal explosion within a confined space, without or with ventilation, the blast load on the structure becomes very complicated due to reflection, re-reflection, and the buildup of the gas pressure ("quasi-static" load). An appropriate simulation of the internal blast must ensure the above

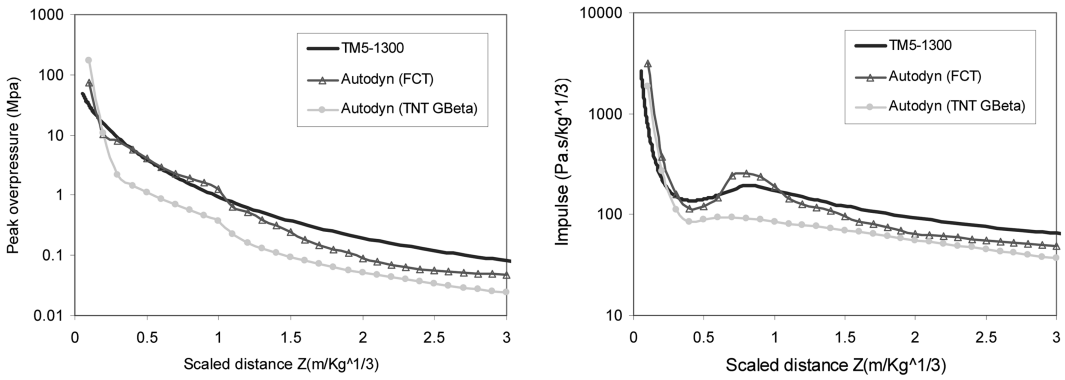

Fig. 5 Comparison of simulated blast load using Autodyn with TM5-1300

processes are adequately reproduced. An examination of adequacy of the reflected shock overpressure also helps to ensure that an effective coupling between the air shock wave and the solid structure is achieved.

For these verification purposes, three different modelling schemes are considered and the corresponding results are compared. The first scheme (model-1) involves a model consisting of only air and a TNT charge, with the enclosure being simulated by fixed boundary planes. This model can provide a benchmark results for comparison since the model settings are quite straightforward and no coupling is required. The second model (model-2) involves explosion in air which is contained in an elastic steel box of 1-m^3. This model necessitates an appropriate coupling treatment between the air and the solid (steel) walls. The configuration for model-3 is similar to model-2 except that a different coupling setting is employed, as will be discussed later. For all the three models, a uniform charge of 1 kg TNT is detonated at the centre of the enclosed space.

The full coupling between the air (fluid, represented by multi-material ALE elements) and solids (represented by Lagrangian elements) in LS-DYNA is achieved through the use of CONSTAINED_LAGRANGE_IN_SOLID keyword which implements a master-slave scheme. Among other factors, an appropriate consideration of the coupling setting and the coupling type is crucial for achieving a realistic coupling simulation. For a proper exchange of data, the mesh grid size of the two meshes at the interface should ideally be kept compatible. To give an idea, in a contact explosion where a dense gird is required for modelling the explosive, Gebbeken *et al.* (1999) recommended a ratio between the Lagrangian and Eulerian mesh gird sizes to be 2~3. However, for the simulation of an airblast-structure system which usually involves a large air domain, it would be difficult to satisfy the above requirement; and our experience tends to show that a configuration with a relatively larger Eulerian grid size than the Lagrangian grid could be acceptable, provided the meshes are sufficiently fine with respect to the propagation of the blast shock wave. Increasing the number of the quadrature points assigned to a surface of each Lagrangian slave segment can be used in place of mesh refinement for fluid-structure interaction simulations. The specification of an insufficient number of quadrature points would generally result in an under-prediction of the energy transferred from the blast onto the structure (due mainly to a significant numerical leakage). On the other hand, increasing the number of quadrature points considerably increases the computational cost. With the the mesh grid size used in the present models, five quadrature points are considered to be appropriate and used for the coupling between the air and the solid structure.

Several coupling types are available in LS-DYNA, for example type 2 which refers to constrained acceleration and velocity (default), and type 5 which implements a penalty based coupling algorithm permitting erosion in the Lagrangian elements. For the applications concerned herein, type 5 coupling scheme appears to be an appropriate choice. The default type 2 coupling is found to be problematic in conserving the system energy during the computation. In the present simulation, model-2 employs type 5 coupling method, while model-3 purposely adopts the default type 2 coupling scheme in order to demonstrate the problem associated with it.

Fig. 6 shows the simulated blast overpressure histories obtained from the three different models. Both model-1 (Eulerian-only model with fixed boundary) and model-2 (type 5 coupling) reproduce a rather realistic internal blast phenomenon, showing clear reflection and re-reflection of the shock waves and gradual build-up of the gas pressure. The peak overpressure at the air-steel interface appears to be higher than at the fixed boundary, and this may be attributable to the dynamic interface effect. On the contrary, the blast load from the simulation with an improper coupling configuration (model-3, type 2 coupling) significantly underestimates the blast load, especially in

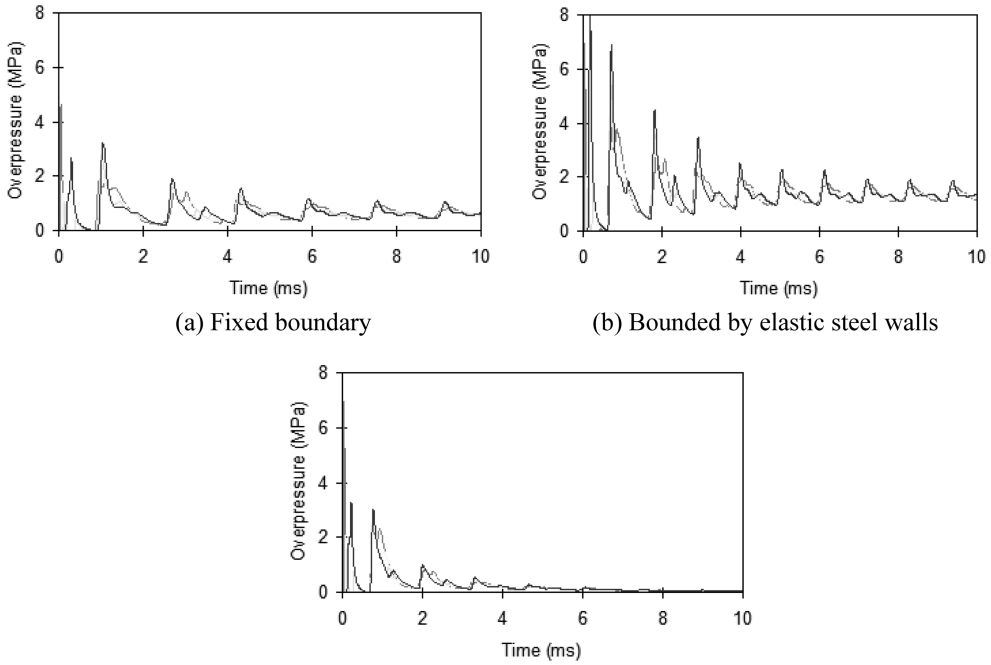

(a) Fixed boundary (b) Bounded by elastic steel walls

(c) Improper coupling (type 2)

Fig. 6 Internal blast load histories from different simulation schemes

terms of the impulse as there is essentially no build-up of the gas pressure due to leakage.

Further examination of the effectiveness of the type 5 coupling scheme will be given in Section 3 in association with the modelling of a physical test.

3. Simulation study on RC response to internal explosion using a coupled model

3.1 General model settings

As a representative case using the fully coupled model, a RC slab subjected to internal explosion is simulated for the calibration and validation of the model considerations. The reasons for choosing this explosion scenario are two folds, a) this scenario involves all the important modelling considerations as would be encountered in a typical case of a concrete component subjected to a close-in explosion, and b) a physical experiment of this type, for which the corresponding author was also involved, is available for comparative observations. The overall experimental programme was reported in Lim and Weerheijm (2006). Fig. 7 shows the computational model configuration.

In the numerical model the explosive charge and air are modeled using the Eulerian solver, while the solid structure including the base box and the slab on the top side of the box are modeled using Lagrangian FE mesh. The Lagrangian and Eulerian meshes are coupled through a validated coupling scheme discussed in Section 2.

To capture the detailed response, for the RC slab the reinforcing bars and concrete are modeled separately by fine brick elements. The reinforcing bars are embedded in the concrete, assuming

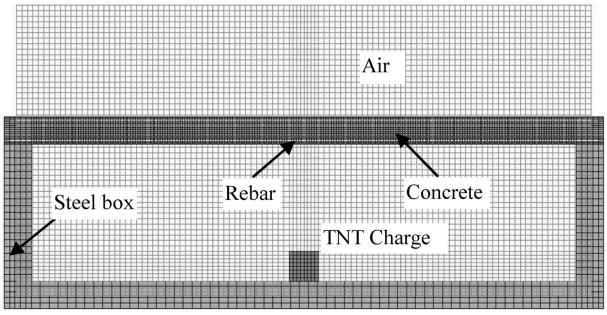

Fig. 7 Coupled computational model for RC slab subjected to internal blast

perfect bond. Because of the high loading rate, the bond-slip mechanism, which would be important in a static or low dynamic loading condition, is deemed to be less significant in the blast response. With a perfect bond, failure at the rebar-concrete interface can still be represented by the failure of the inner layer of concrete joined to the rebar surface.

The reinforcing bars are modeled as elastoplastic. The strain rate effect is considered by imposing a dynamic increase factor on the strength according to the formula proposed by Malvar (1998)

$$\frac{f_d}{f_S} = \left(\frac{\dot{\varepsilon}}{10^{-4}}\right)^{\alpha}$$

where for the yield stress, $\alpha = 0.074 - 0.04\frac{f_y}{414}$, with f_y being the static yield strength of the material.

For the modelling of concrete material under shock and blast loading, there exist a number of options (see for example Tu and Lu 2009). In the present study, the K&C model (or Concrete Damage Model as referred to in LS-DYNA) (Malvar *et al.* 1997, 2000) is employed. This model is capable of describing the concrete behaviour under complex stress and high pressure conditions. For the strain rate effect of concrete, the CEB-FIP model (1993) is adopted.

The K&C concrete model implements three strength surfaces, namely an initial yield surface, a maximum failure surface and a residual surface, and all the three stress invariants (I_1, J_2 and J_3) are

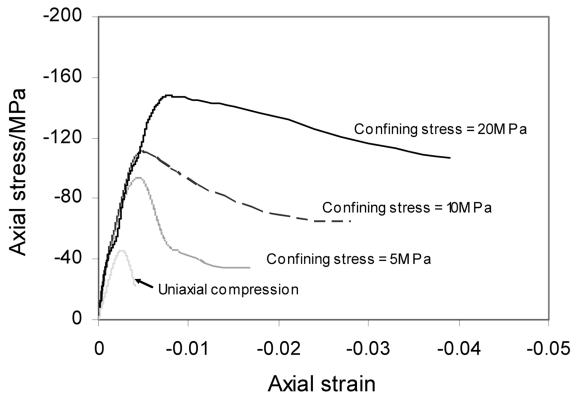

Fig. 8 Unconfined and confined compression stress-strain relationships generated by the Concrete Damage model

involved in defining the strength surfaces. A damage function λ, which is related to both the effective plastic strain and the hydrostatic pressure, is defined to control the softening behaviour of the material. To illustrate the behaviour of the model, Fig. 8 shows a set of compressive stress-strain curves generated using a single FE element with the present concrete model, for different levels of lateral confining stresses. The trend of increase of the ductility and strength with increase of the confinement agrees well with the general experimental observations.

In addition to the damage model, a piece-wise approximation of the equation of state is used to describe the compaction for the concrete material.

3.2 Simulation of concrete crack with erosion

In order to simulate the physical separation of concrete due to crack opening in the numerical model, the so-called "erosion" algorithm is adopted. When the material response in an element reaches a pre-defined limit so that the element may be considered as failed, the element is physically deleted from the computational model. The deletion of elements forms discontinuity that resembles macro cracks in the structure. The deletion process is irreversible; therefore it would only be rational to consider such a technique for crack simulation when the response is dominated by a monotonic process, such as the response during the direct blast load. It is worth noting that the erosion of elements results in a loss of mass, and thus a loss of energy and momentum in the entire system. However, by taking into account (subtracting) such losses in the calculations, they should not introduce problems in terms of energy balance in the updated system.

A variety of criteria may be considered to control the erosion. For the simulation of crack induced discontinuity, the use of tensile strain as a criterion for erosion is a reasonable choice. The limit strain value may be deduced as follows (Xu and Lu 2006). Consider for typical concrete the strain at peak tensile stress to be around 0.0002 (one-tenth of that at peak compressive stress) for static loading. After a softening phase, the tensile strain for macro cracking is expected to be a few times of the above peak strain value, to the order of 0.001. Under direct blast loading, the strain rate in concrete is usually very high (say 100/s for an indicative purpose), the dynamic tensile strength can thus increase by several times from the static tensile strength. Although there is no systematic experimental evidence to indicate a proportional increase in the dynamic strain, it is reasonable to expect a general increase in the fracture strain limit under high rate loading. For these reasons, it is proposed that a dynamic strain limit for macro cracking be set in a range of 0.002 to 0.01.

It should be emphasized again that such a limit strain is applicable only in cases where cracking and global expansion are the dominant phenomena in the process. For responses involving crushing of concrete due to compression or combined stresses, such as in the case of projectile penetration, the erosion limit will have to be determined accordingly, and this is often for the purpose to avoid severe mesh distortion rather than for the physical state of the material.

3.3 Simulation results of RC Slab response to internal explosion

The coupled computational model and the material models described above are applied in the simulation of a representative RC slab under internal explosion. The dimensions of the RC slab follow the physical experiment, being 2 m (length) × 1 m (width) × 0.1 m (thickness). The slab is clamped along its two shorter sides to a rectangular steel chamber, so as to resemble a one-way slab condition. The explosive charge is placed at the bottom of the chamber, as shown in Fig. 7, and

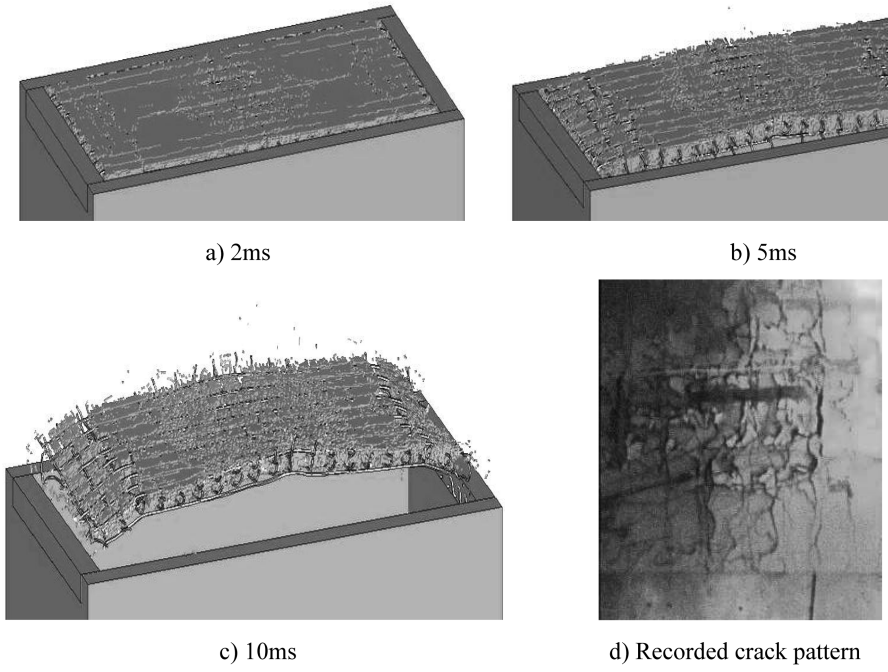

Fig. 9 Evolution of concrete fracture and break-up under internal blast

detonated to generate the internal blast load on the RC slab. During the actual experiments, explosions with different charge weights, ranging from 0.5 to 4 kg, were tested. In the present simulation, a model charge of 2.0 kg TNT is considered, and this model charge may be regarded as representing a real TNT charge of approximately 1.0 kg in accordance with the blast calibration results described in Section 2.

In the model, over 350,000 Eulerian elements are used to model the TNT explosive charge and the air medium, while about 360,000 Lagrangian finite elements are used to model concrete and steel bars. The concrete is assumed to have the following properties: compressive strength = 40 MPa, Young's modulus = 27 GPa, Poisson's ratio = 0.2, and a uniaxial tensile strength 4 MPa. The yield strength of the steel bars is assumed to be 460 MPa. An erosion strain limit of 0.002 is used to simulate cracking in the concrete. The rupture limit strain for the steel bars is set at 0.15.

The development of cracking in the RC slab during the response is shown in Fig. 9. The response can be generally divided into three stages. At the beginning (within the first 2 ms herein), the slab exhibits cracks on the top surface and they clearly follow the rebar grids. This is attributable to the shock wave effect, wherein the overall displacement of the slab remains small. At the second stage, the slab responds into the global modes, whereby flexural cracks develop, along with shear failure near the two support ends (at around 5 ms herein). Finally, the slab breaks away as a free body due to shearing off at the two supporting ends, while the material tends to disintegrate into debris (held only by the reinforcing bars). This response process agrees well with the observations from the experiment.

It is noteworthy that the initial fracture pattern, which appears to have formed within the first 2 ms while the loading is dominated by the shock wave, provides a characteristic pattern of the final crack distribution. This observation tends to support the view (Brinkman 1987, Simha *et al.* 1987)

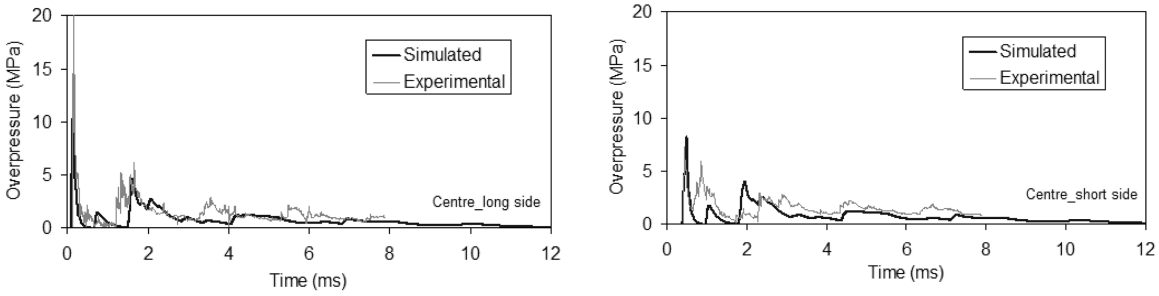

(a) At centre of side wall (b) At centre of end wall

Fig. 10 Air overpressure time histories inside the chamber (on vertical walls)

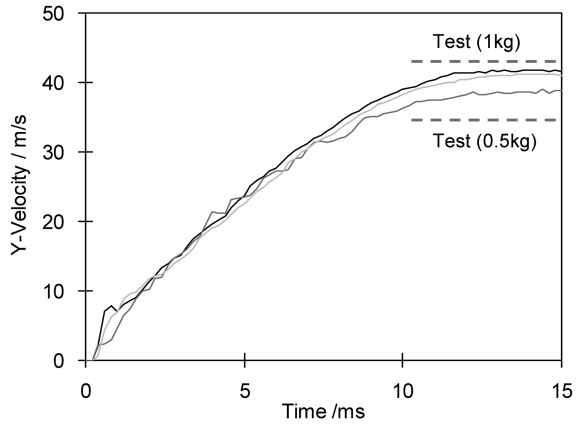

Fig. 11 Velocity of the RC slab at selected points

that in an internal blast environment the shock wave loading is responsible for the development of damage zone in the concrete material, while explosion gas loading is important in the separation of cracks and in the subsequent throw of the fragments.

The air overpressure time histories from the simulation, recorded at two representative locations inside the chamber, are depicted in comparison with the experimental data in Fig. 10. A favourable agreement is observed. The computed waveform of the overpressure shows similar characteristic features as the experimental counterpart, including the reflection of the overpressure and emergence of the gaseous loading phase. It is worth noting that the gas loading phase appears to vanish after about 10 ms, and this is reasonable because, as can be seen from Fig. 9, the slab at this time is completely separated from the test box, resulting in the escape of the explosive gas and hence the dying out of the gas pressure.

The velocity of the slab debris also serves as an important indicator of the adequacy of the overall model setting, as it represents the (kinetic) energy that the blast load imparts to the responding slab. Fig. 11 shows a comparison of the simulated debris launch velocities with the measured counterparts from two tests. It can be seen that the simulated results agree favourably with the 1.0 kg test data.

Summarizing the above simulation results and comparison with the experimental observations, it can be clearly seen that the coupled computational model performs satisfactorily for the simulation

of the entire blast load and the structural response processes. The general agreement between the simulation results and the experimental data, both in terms of the internal blast and the dynamic response of the RC slab, tends to support the blast load calibration such that a charge enhancement factor on the order of 2 may be considered for the simulation of close-in blast concerning the structural effect.

4. Simulation study on RC column response to open air blast using a coupled model

To represent a more generic explosion scenario, a RC column subjected to close-in air blast is simulated using the coupled Eularian-Lagrangian modeling approach. The column has the following properties: length = 4 m, cross-section = 0.4 × 0.4 m, longitudinal reinforcement = 4 bars of 16 mm dia. with yield strength 460 MPa, stirrups = 10 mm dia. at 200 mm spacing with yield strength 260 MPa. The concrete has a characteristic compressive strength of 40 MPa. The column is fully fixed at both top and bottom ends.

The column is analyzed under a high explosive charge of 10 kg TNT (equivalent) located at 1m from the front face of the column, and at 1m above the ground surface. This explosion scenario is expected to be enough to generate substantial damage to the column, but not necessarily results in a total failure. Based on the calibration results mentioned in Section 3, in the actual simulation the charge is modelled by a 20-kg TNT rectangular mass.

Two different mesh schemes are considered, one featured by a 20-mm brick elements for the RC column (model-A), and another with a further refined 10-mm brick elements for the RC column (model-B). Model-B has a total number of over 500,000 solid elements for the RC column alone. In both models, the macro cracks are simulated by element erosion with an erosion criterion of principal tensile strain reaching 0.002. To check the model sensitivity to the erosion limit, Model-B is also analyzed using a conservative erosion limit of 0.01.

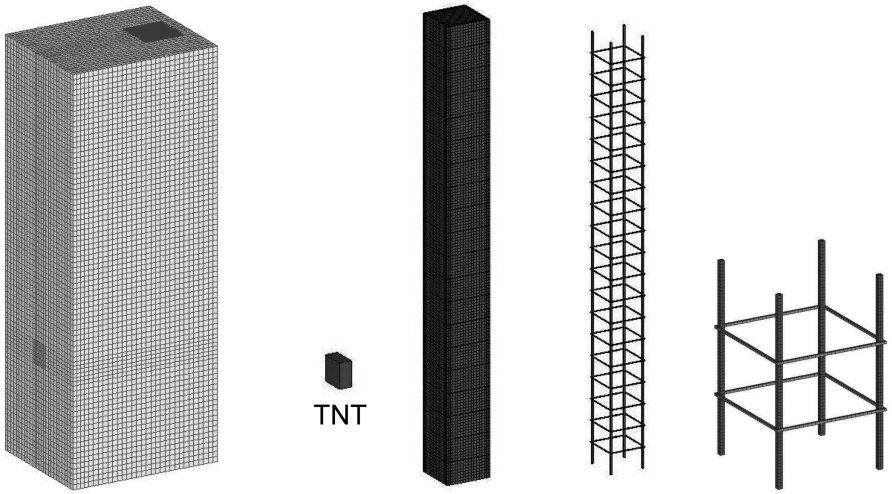

(a) Coupled model domains (b) Column and TNT (c) Reinforcing bars

Fig. 12 Model configuration for RC column subjected to close-in explosion

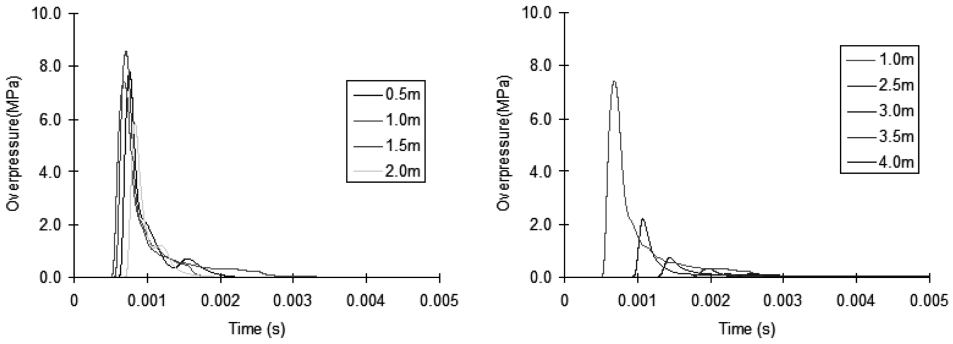

Fig. 13 Blast load histories measured on the front face of column, at different heights

Fig. 12 shows the model configuration. The entire RC column is surrounded by a volume of air. Considering symmetry about the vertical central plane viewing from the front, only half of the space shown in Fig. 12(a) is actually modelled. Apart from the symmetrical plane, the air medium is fixed at the bottom to simulate the ground reflection, while it is truncated at all other sides with a non-reflection boundary to mimic air flow to the outside air medium. At the interface between the air and the column faces, the two meshes are fully coupled in the normal direction. The grid size for the air is about twice the nominal size of the solid elements.

Fig. 13 shows the blast load histories recorded at eight locations on the front face of the column along the height. It can be clearly observed that in an explosion scenario with a small standoff distance, in the current case being 1 m or 1-4th of the column height, the spatial distribution of the blast load on a structural component varies significantly. The highest loading density, both in terms of the peak overpressure and the impulse, takes place in the locations nearest to the charge centre, whereas at the farthest end of the column, the blast load drops to an order of magnitude lower. Therefore, it is important that such a spatial variation of the blast load is taken into account if the load is imposed directly on the structural member without using a coupled model.

The variation of the blast load along the height of the column produces a distinctive damage pattern, which may be characterized by severe material failure modes (spalling and cracking) in the lower part of the column, followed by distributed cracking due to global bending and shearing. Figs. 14 and 15 show the progressive damage patterns from Model-A and Model-B, respectively, with an erosion strain limit of 0.002. It can be observed that the two sets of damage patterns are comparable and show similar global characteristics. The main difference resulted from increasing the mesh density for the concrete column, i.e. from 20 mm for Model-A to 10-mm for model-B (at the cost of increasing the total number of elements by 8 times) lies in the details of the crack distributions, with model-B exhibiting more spread bending and shearing cracks. This comparison suggests that as far as the general response is concerned, using a mesh resolution of order of 20 mm for the concrete column may be acceptable for short standoff blast response simulations.

Increasing the erosion strain limit from 0.002 to 0.01, as can be observed from Fig. 15 in comparison with Fig. 16, does not appear to affect significantly the global response in terms of the displacement and overall damage, but does affect quite markedly the distribution of visible cracks. This is expected since the increase of the erosion strain will directly delay and reduce the element deletion, and hence the discontinuities. The reason why the global response is relatively insensitive to the erosion limit, on the other hand, may be attributed to the soundness of the material model

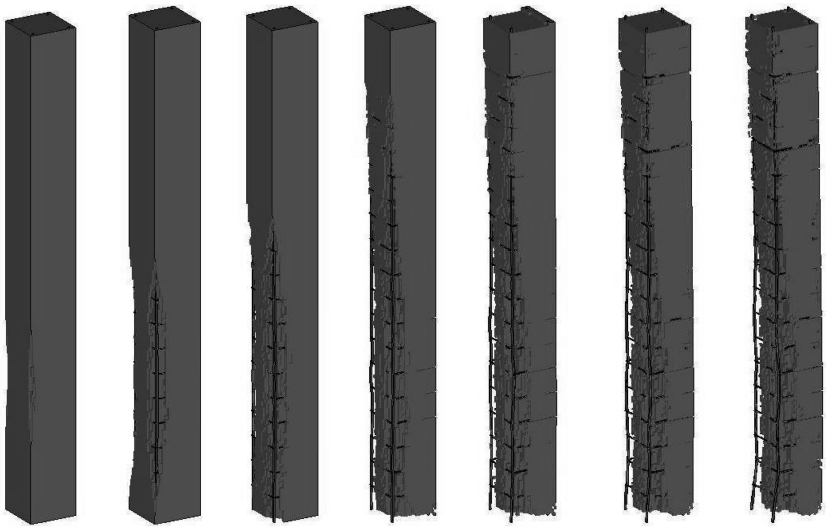

(From left to right) 0.06, 0.08, 1, 2, 5, 10, 20 ms after detonation

Fig. 14 Progress of damage of Model-A (20-mm concrete elements)

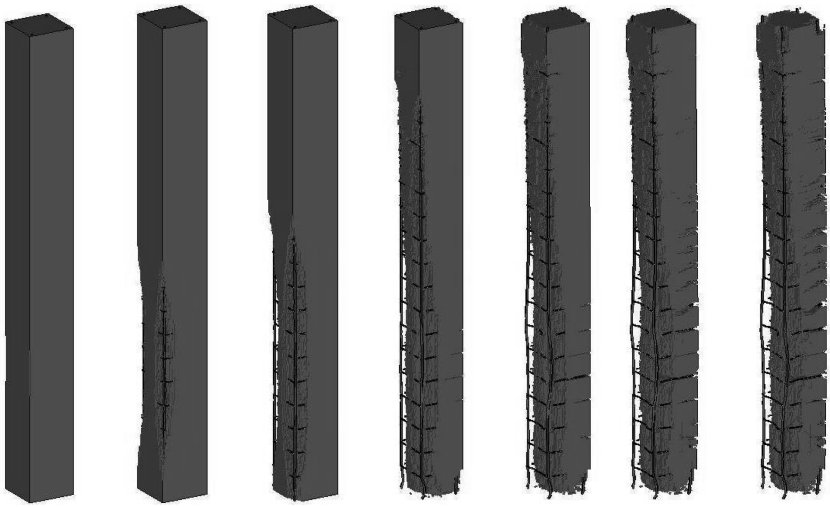

(From left to right) 0.06, 0.08, 1, 2, 5, 10, 20 ms after detonation

Fig. 15 Progress of damage of Model-B (10-mm concrete elements)

used for concrete in the present study. As a matter of fact, in such a concrete material model the accumulation of damage will reach a value close to unity before the above prescribed erosion strain limit is attained. As a result, the respective element(s) will have only a minimal contribution towards the bulk material response even if they are not deleted. Bearing this in mind, it may be rational to adopt a safer (higher) erosion limit so as to minimize the risk of running into a premature disintegration failure, provided a sound material model is in place.

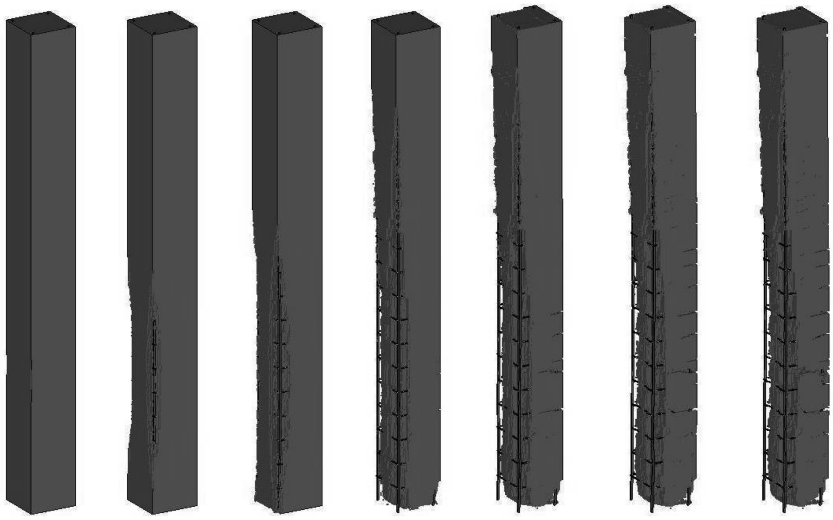

(From left to right) 0.06, 0.08, 1, 2, 5, 10, 20 ms after detonation

Fig. 16 Progress of damage of Model-B with erosion limit increased from 0.002 to 0.01

5. Conclusions

A series of calibration and validation study is presented on the simulation of RC structural components subjected to close-in blast using a coupled computational model. The model incorporates a Lagrangian finite element description of the solid structure, and an Eulerian description of the explosion charge and the air medium. The calibration covers three important aspects in such coupled modelling applications, namely the blast load, the mesh sensitivity, and the use of different erosion limits for the simulation of macro cracking.

The calibration of the simulated blast load is carried out first in free air, for which empirical data exist in the existing literature. The results indicate that the simulated blast load is rather sensitive to the mesh grid size, and the results tend to improve with increase of the mesh density. However, in general the simulated blast load using the 3D Eulerian solver in LS-DYNA appears to be consistently lower than the empirical predictions, by a factor on the order of 2 in terms of the charge weight. To some extent, using the FCT technique in AUTODYN appears to yield a more satisfactory blast load simulation, especially in the close-in range (up to about 1 $m/kg^{1/3}$). These observations highlight the need of having a dedicated blast load calibration when a coupled model is to be employed for a comprehensive numerical investigation, so as to ensure a reliable interpretation of the results.

The validation study on the simulation of the RC slab under internal explosion indicates that, with an adequate coupling scheme, a realistic internal blast environment can be reproduced that encompasses the shock re-reflection effect as well as the build-up of the gas pressure. In conjunction with appropriate material models and an adequate use of the erosion technique, it is possible to reproduce the characteristic crack patterns and the global response using a coupled model. It is argued that for cases which are dominated by a monotonic and tension-dominated process, a tensile strain limit in the range of 0.002-0.01 may be appropriate. The above erosion

strain limit for cracking is further supported by the simulation of a typical RC column subjected to open air blast. A variation of the erosion limit in the above range does not seem to alter the characteristic crack patterns; however, the detailed crack distributions may be affected.

The simulation studies carried out on the RC slab and column cases also indicate that for a high fidelity simulation of RC response to close-in blast, a mesh grid size of order 10-20 mm may be required due to the drastic spatial distribution of the stress wave effect. As this level of spatial resolution actually falls into the scale of meso-level heterogeneity of concrete material, the subject of material heterogeneity comes into picture.

References

AUTODYN (2001), v4.2 manual, Century Dynamics, Inc.

Baker, W.E. (1973), *Explosions in Air*, University of Texas Press, Austin, TX.

Brinkman, J.R. (1987), "Separating shock wave and gas expansion breakage mechanisms", *Proceeding of the Second International Symposium on Rock Fragmentation by Blasting*, Colorado, Keystone, 6-15.

CEB-FIP (1993), Comite Euro-International du Beton, CEB-FIP Model Code 1990. Redwood Books, Trowbridge, Wiltshire, UK.

Gatuingt, F. and Pijaudier-Cabot, G. (2002), "Coupled damage and plasticity modeling in transient dynamic analysis of concrete", *Int. J. Numer. Anal. Meth. Geomech.*, **26**, 1-24.

Gebbeken, N. and Ruppert, M. (2000), "A new material model for concrete in high-dynamic hydrocode simulations", *Arch. of Appl. Mech.*, **70**, 463-478.

Gebbeken, N. and Ruppert, M. (1999), "On the safety and reliability of high dynamic hydrocode simulations", *Int. J. Numer. Meth. Eng.*, **46**, 839-851.

Gong, S. and Lu, Y. (2007), "Combined continua and lumped parameter modelling for nonlinear response of structural frames to impulsive ground shock", *J. Eng. Mech.*, ASCE, **133**(11), 1229-1240.

Henrych, J. (1979), *The Dynamics of Explosion and Its Use*, Elsevier Scientific Publishing Company, New York.

Holmquist, T.J., Johnson, G.R. and Cook, W.H. (1993), "A computational constitutive model for concrete subjected to large strain, high strain rates and high pressures", *14th International Symposium on Ballistics*, Quebec, Canada, 591-600.

Hommert, P.J., Kuszmaul, J.S. and Parrish, R.L. (1987), "Computational and experimental studies of the role of stemming in cratering", *Proceeding of the Second International Symposium on Rock Fragmentation by Blasting*, Colorado, Keystone, 550-562.

Krauthammer, T., Frye, M., Schoedel, T.R. and Seltzer, M. (2003), "Advanced SDOF approach for structural concrete systems under blast and impact loads", *11th Int. Sym. on the Interaction of the Effects of Munitions with Structures*, Mannheim, Germany.

Lee, E.L., Hornig, H.C. and Kury, J.W. (1968), "Adiabatic expansion of high explosive detonation products", UCRL-50422, Lawrence Radiation Laboratory, University of California.

Leppanen, J. (2006), "Concrete subjected to projectile and fragment impacts: Modelling of crack softening and strain rate dependency in tension", *Int. J. Impact Eng.*, **32**, 1828-1841.

Lim, H.S. and Weerheijm, J. (2006), "Breakup of concrete slab under internal explosion", 32nd DoD Explosives Safety Seminar, Philadelphia, PA.

LS-DYNA (2003), *Keyword User's Manual*, Version 970. Livermore Software Technology Corporation.

Malvar, L.J., Crawford, J.E. and Morrill, K.B. (2000), "K&C concrete material model Release III—Automated generation of material model input", K&C Technical Report TR-99-24-B1.

Malvar, L.J. (1998), "Review of static and dynamic properties of steel reinforcing bars", *ACI Mater. J.*, **95**(5), 609-616.

Malvar, L.J., Crawford, J.E., Wesevich, J.W. and Simons, D. (1997), "A plasticity concrete material model for DYNA3D", *Int. J. Impact Eng.*, **19**(9-10), 847-873.

Rabczuk, T. and Eibl, J. (2006), "Modelling dynamic failure of concrete with meshfree methods", *Int. J. Impact*

Eng., **32**, 1878-1897.
TM5-1300 (1990), *Structures to Resists the Effects of Accidental Explosions*. Department of the Army. USA.
Tu, Z. and Lu, Y. (2009), "Evaluation of typical concrete material models used in hydrocodes for high dynamic response simulations", *Int. J. Impact Eng.*, **36**, 132-146.
Xu, K. and Lu, Y. (2006), "Numerical simulation study of spallation in reinforced concrete plates subjected to blast loading", *Comput. Struct.*, **84**(5-6), 431-438.